1. AGENCY USE ONLY (Leave blank)	2. REPORT DATE	3. REPORT TYPE AND DATES COVERED
	February 1993	professional paper

4. TITLE AND SUBTITLE

EFFECTS OF MISALIGNMENT ON PROPAGATION CHARACTERISTICS OF TRANSMISSION LINES PRINTED ON ANISOTROPIC SUBSTRATES

5. FUNDING NUMBERS

In-house funding

6. AUTHOR(S)

T. Q. Ho and B. Beker

7. PERFORMING ORGANIZATION NAME(S) AND ADDRESS(ES)

Naval Command, Control and Ocean Surveillance Center (NCCOSC)
RDT&E Division
San Diego, CA 92152–5001

8. PERFORMING ORGANIZATION REPORT NUMBER

9. SPONSORING/MONITORING AGENCY NAME(S) AND ADDRESS(ES)

Naval Command, Control and Ocean Surveillance Center (NCCOSC)
RDT&E Division
Block Programs
San Diego, CA 92152–5001

10. SPONSORING/MONITORING AGENCY REPORT NUMBER

11. SUPPLEMENTARY NOTES

12a. DISTRIBUTION/AVAILABILITY STATEMENT

Authorized for public release; distribution is unlimited.

12b. DISTRIBUTION CODE

13. ABSTRACT (Maximum 200 words)

The spectral-domain method is applied to study the propagation characteristics of grounded transmission lines on biaxial substrates whose axes are misaligned with those of the line. The three structures under investigation are the grounded slotline, microstrip, and the edge coupled line. The formulation derives an expression for the Green's function that is valid for substrates which are simultaneously characterized by both their permittivity and permeability tensors. The off-diagonal elements of the permittivity tensor, present due to the misalignment of the axes, are used to examine the dispersion properties of these transmission lines with numerous case-studies presented for different angles of rotation.

Published in *IEEE Transactions on Microwave Theory and Techniques*, Vol. 40, No. 5, May 1992.

14. SUBJECT TERMS	15. NUMBER OF PAGES
Green's function propagation biaxial substrates	16. PRICE CODE

17. SECURITY CLASSIFICATION OF REPORT	18. SECURITY CLASSIFICATION OF THIS PAGE	19. SECURITY CLASSIFICATION OF ABSTRACT	20. LIMITATION OF ABSTRACT
UNCLASSIFIED	UNCLASSIFIED	UNCLASSIFIED	SAME AS REPORT

21a NAME OF RESPONSIBLE INDIVIDUAL	21b TELEPHONE (Include Area Code)	21c OFFICE SYMBOL
T. Q. Ho	(619) 553-3783	Code 824

waves," and "Reply" by P. Overfelt and D. J. White, *IEEE Trans. Microwave Theory Tech.*, vol. 39, pp. 612–614, Mar. 1991.
[2] P. L. Overfelt and D. J. White, "TE and TM modes of some triangular cross-section waveguides using superposition of plane waves," *IEEE Trans. Microwave Theory Tech.*, vol. MTT-34, pp. 161–164, Jan. 1986.
[3] S. A. Schelkunoff, *Electromagnetic Waves*. New York: Van Nostrand, 1943, pp. 393–397.
[4] M. G. Lame', *Lecons sur la Theorie Mathematique de l'Elasticite des Corps Solides*. Paris: Bachelier, 1852.
[5] M. A. Pinsky, "The eigenvalues of an equilateral triangle," *SIAM J. Math. Anal.*, vol. 11, pp. 819–827, Sept. 1980.
[6] P. M. Morse and H. Feshbach, *Methods of Theoretical Physics, Part I*. New York: McGraw-Hill, 1953, pp. 754–757.
[7] W. J. LeVeque, *Topics in Number Theory*. Reading, MA: Addison-Wesley, 1956, vol. II, Ch. 1.
[8] B. W. Jones, *Arithmetic Theory of Quadratic Forms*. New York: Wiley, 1950.
[9] G. H. Hardy and E. M. Wright, *An Introduction to the Theory of Numbers*. Oxford: Clarendon, 1938.
[10] A. Clark, *Elements of Abstract Algebra*. New York: Dover, 1984.

Effects of Misalignment on Propagation Characteristics of Transmission Lines Printed on Anisotropic Substrates

T. Q. Ho and B. Beker

***Abstract*—The spectral-domain method is applied to study the propagation characteristics of grounded transmission lines on biaxial substrates whose axes are misaligned with those of the line. The three structures under investigation are the grounded slotline, microstrip, and the edge coupled line. The formulation derives an expression for the Green's function that is valid for substrates which are simultaneously characterized by both their permittivity and permeability tensors. The off-diagonal elements of the permittivity tensor, present due to the misalignment of the axes, are used to examine the dispersion properties of these transmission lines with numerous case-studies presented for different angles of rotation.**

I. Introduction

Recently, transmission lines on anisotropic materials have become increasingly more attractive in microwave and millimeter-wave integrated circuit applications. Different types of guiding structures such as the microstrip line, coupled line, finline, and slotline on simple anisotropic substrates have been extensively studied by numerous authors in the past. Since the early work on microstrips printed on sapphire substrates, which was presented by Owens *et al.* [1], many other transmission lines on such materials have also been examined in detail. Included among these studies is an open sidewall microstrip which was analyzed by the hybrid mode approach, described by El-Sherbiny [2]. In addition, propagation characteristics of single as well as coupled lines on planar anisotropic layers were also examined via the method of moments, as documented by Alexopoulos *et al.* [3]. Other researchers, such as Nakatani *et al.* [4], have extended the full-wave analysis to study suspended structures, while Yang *et al.* [5] have examined the dispersive properties of a finline. In all of the aforementioned works, however, the anisotropy of a substrate was represented by a diagonal permittivity tensor only.

Up until now, there have been only a few studies dealing with effects of misalignment between the axes of the substrate and those of the waveguide on the dispersive characteristics of transmission lines printed on anisotropic materials. Mathematically, such effects are included by the presence of the off-diagonal elements in the permittivity tensor. Most of the research efforts, thus far, have been primarily focused on open transmission lines, with the most general treatment available in [6]. Therein, Tsalamengas *et al.* have considered an open microstrip line with a substrate which is characterized by generalized $[\epsilon]$ and $[\mu]$ tensors. In their analysis they used a complicated semi-analytical method, however, they did not provide any numerical results for the effects of misalignment on the dispersive properties of the structure. On the other hand, for shielded structures, and specifically for edge coupled lines on a boron nitride, Mostafa *et al.* [7] used a full-wave solution to calculate their dispersion properties for dominant as well as higher order modes.

In this paper, a full-wave analysis applying the spectral-domain technique is used to analyze the effects of misalignment on the propagation characteristics of grounded slotlines, microstrip line, and edge coupled lines printed on biaxial substrates. The material can be characterized simultaneously by both permittivity and permeability tensors, with the rotation of the principal axes restricted to the permittivity tensor alone. Numerical results for various transmission lines are examined in detail with respect to different physical dimensions of the structure, substrate parameters, and angles of rotation of the principal axes of the permittivity tensor.

II. Theory

The specific transmission line structures under consideration are shown in Figs. 1, 2, and 3 along with the coordinate system used to formulate the problem. All metal strips are assumed to be perfectly conducting and infinitely thin. The substrate, whose thickness is h_1, is lossless and is characterized by its permittivity and permeability tensors

$$[\epsilon] = \epsilon_o \begin{bmatrix} \epsilon_{xx} & \epsilon_{xy} & 0 \\ \epsilon_{yx} & \epsilon_{yy} & 0 \\ 0 & 0 & \epsilon_{zz} \end{bmatrix} \quad \text{and} \quad [\mu] = \mu_o \begin{bmatrix} \mu_{xx} & 0 & 0 \\ 0 & \mu_{yy} & 0 \\ 0 & 0 & \mu_{zz} \end{bmatrix} \tag{1a}$$

with elements of the relative $[\epsilon]$ given by

$$\epsilon_{xx} = \epsilon_2 \sin^2(\theta) + \epsilon_1 \cos^2(\theta),$$
$$\epsilon_{yy} = \epsilon_2 \cos^2(\theta) + \epsilon_1 \sin^2(\theta)$$
$$\epsilon_{zz} = \epsilon_3,$$
$$\epsilon_{xy} = \epsilon_{yx} = (\epsilon_2 - \epsilon_1) \sin(\theta) \cos(\theta) \tag{1b}$$

where ϵ_o and μ_o are the free-space permittivity and permeability, respectively. The angle θ is the rotation angle of the x and y principal axes of the tensor with respect to the x and y coordinate axes of the structure about the common z-axis.

The vector wave equations for the components of the electric and

Manuscript received August 22, 1991; revised December 11, 1991.
T. Q. Ho was with the Department of Electrical and Computer Engineering, University of South Carolina, Columbia, SC 29208. He is presently with the NCCOSC, RDT&E Division, San Diego, CA 92152.
B. Beker is with the Department of Electrical and Computer Engineering, University of South Carolina, Columbia, SC 29208.
IEEE Log Number 9106764.

magnetic fields within the biaxial substrate can be written in their compact forms as

$$\nabla \times ([\mu]^{-1} \cdot \nabla \times \mathbf{E}) - k_o^2[\epsilon] \cdot \mathbf{E} = 0 \tag{2a}$$

$$\nabla \times ([\epsilon]^{-1} \cdot \nabla \times \mathbf{H}) - k_o^2[\mu] \cdot \mathbf{H} = 0, \tag{2b}$$

where the relative $[\epsilon]$ and $[\mu]$ were previously defined in (1), and k_o is the free-space wave number.

The Fourier transform of any field component within the housing is defined via the following integral relation

$$\bar{F}(x, \alpha) = \int_{-b/2}^{b/2} F(x, y)\, e^{j\alpha y}\, dy \tag{3a}$$

$$\alpha = (2n - 1)/b \tag{3b}$$

with α being the discrete Fourier transform variable and with b being the dimension of the broad sidewall of the waveguide. When (2a) and (2b) are simplified, they can be reduced to a set of scalar coupled differential equations for $\bar{E}_y$ and $\bar{E}_z$ which are given by

$$\frac{d^2\bar{E}_y(x, \alpha)}{dx^2} y_1 \frac{d\bar{E}_y(x, \alpha)}{dx} + y_2\bar{E}_y(x, \alpha) + y_3 \frac{d\bar{E}_z(x, \alpha)}{dx} + y_4\bar{E}_z(x, \alpha) = 0 \tag{4a}$$

$$\frac{d^2\bar{E}_z(x, \alpha)}{dx^2} + z_1 \frac{d\bar{E}_z(x, \alpha)}{dx} + z_2\bar{E}_z(x, \alpha) + z_3 \frac{d\bar{E}_z(x, \alpha)}{dx} + z_4\bar{E}_y(x, \alpha) = 0 \tag{4b}$$

with all coefficients appearing above defined as

$$y_1 = \frac{-j\alpha\epsilon_{xy}}{\epsilon_{xx}} + j\alpha(\mu_{zz}/\mu_{xx}) \frac{\{k_o^2\mu_{xx}\epsilon_{yx} - \alpha^2(\mu_{xx}\epsilon_{yx}/\mu_{zz}\epsilon_{xx})\}}{\{\alpha^2 + \beta^2(\mu_{zz}/\mu_{yy}) - k_o^2\mu_{zz}\epsilon_{xx}\}} \tag{4c}$$

$$y_2 = -\alpha^2 \frac{\epsilon_{yy}}{\epsilon_{xx}} - \beta^2 \frac{\mu_{zz}}{\mu_{xx}} + k_o^2\mu_{zz}\zeta_y \tag{4d}$$

$$\zeta_y = \epsilon_{yy} + \frac{\mu_{zz}\epsilon_{xy}\{k_o^2\mu_{xx}\epsilon_{yx} - \alpha^2(\mu_{xx}\epsilon_{yx}/\mu_{zz}\epsilon_{xx})\}}{\mu_{xx}\{\alpha^2 + \beta^2(\mu_{zz}/\mu_{yy}) - k_o^2\mu_{zz}\epsilon_{xx}\}} \tag{4e}$$

$$y_3 = \frac{j\beta\mu_{zz}^2}{\mu_{xx}\mu_{yy}} \frac{\{k_o^2\mu_{xx}\epsilon_{yx} - \alpha^2(\mu_{xx}\epsilon_{yx}/\mu_{zz}\epsilon_{xx})\}}{\{\alpha^2 + \beta^2(\mu_{zz}/\mu_{yy}) - k_o^2\mu_{zz}\epsilon_{xx}\}} \tag{4f}$$

$$y_4 = \beta\alpha \frac{\mu_{zz}\{1 - (\mu_{xx}\epsilon_{zz}/\mu_{zz}\epsilon_{xx})\}}{\mu_{xx}} \tag{4g}$$

$$z_1 = \frac{-j\alpha\beta^2\epsilon_{yx}\mu_{zz}}{\epsilon_{xx}\mu_{yy}\{\alpha^2 + \beta^2(\mu_{zz}/\mu_{yy}) - k_o^2\mu_{zz}\epsilon_{xx}\}} \tag{4h}$$

$$z_2 = k_o^2\mu_{yy}\epsilon_{zz} - \alpha^2(\mu_{yy}/\mu_{xx}) - \beta^2(\epsilon_{zz}/\epsilon_{xx}) \tag{4i}$$

$$z_3 = \frac{-j\beta\epsilon_{xy}}{\epsilon_{xx}} - \frac{j\beta\alpha^2\epsilon_{yx}}{\epsilon_{xx}\{\alpha^2 + \beta^2(\mu_{zz}/\mu_{yy}) - k_o^2\mu_{zz}\epsilon_{xx}\}} \tag{4j}$$

$$z_4 = \alpha\beta\left\{\frac{\mu_{yy}}{\mu_{xx}} - \frac{\epsilon_{yy}}{\epsilon_{xx}} - \zeta_z\frac{\epsilon_{yx}}{\epsilon_{xx}}\right\} \tag{4k}$$

$$\zeta_z = \frac{k_o^2\mu_{zz}\epsilon_{xy}}{\alpha^2 + \beta^2(\mu_{zz}/\mu_{yy}) - k_o^2\mu_{zz}\epsilon_{xx}}, \tag{4l}$$

where β is the propagation constant in the z-direction.

To find the solution for either $\bar{E}_y$ or $\bar{E}_z$, (4a) and (4b) can be decoupled yielding a fourth order differential equation for either component of the electric field. The remaining field components in the planar anisotropic region are then obtained from Maxwell's equations in terms of $\bar{E}_z$ (as shown in [11]), whose explicit expression is written below

$$\bar{E}_z(x, \alpha) = A_n^* \sin(\gamma_x x) + B_n^* \sin(\gamma_x x) \tag{5}$$

with (γ_x) denoting the propagation constants of fields in the anisotropic region 1 along the x direction, A_n^* and B_n^* corresponding to the modal amplitudes of $\bar{E}_z$, and ω being the angular frequency. The propagation constants (γ_x) may be obtained by solving a fourth order characteristic equation for either $\bar{E}_y$ or $\bar{E}_z$, and expressed in terms of α, β, as well as the medium parameters of the substrate.

The fields inside the isotropic region 2 can be derived with the help of the potential theory. In general, the governing equations for the two potential functions within this region can be written in terms of $\phi^{e,h}$ which denote the potential functions for the TM and TE modes, respectively [5].

By applying the boundary conditions at the air-anisotropic layer interface, i.e., at $x = h_1$ a set of matrix equations can be obtained, which yields an expression for the admittance Green's function given below

$$\begin{bmatrix} \bar{Y}_{yy}(\alpha, \beta) & \bar{Y}_{yz}(\alpha, \beta) \\ \bar{Y}_{zy}(\alpha, \beta) & \bar{Y}_{zz}(\alpha, \beta) \end{bmatrix} \begin{bmatrix} \bar{E}_y(h_1, \alpha) \\ \bar{E}_z(h_1, \alpha) \end{bmatrix} = \begin{bmatrix} J_y(\alpha) \\ J_z(\alpha) \end{bmatrix} \tag{6a}$$

whose individual matrix elements are defined by

$$\bar{Y}_{yy}(\alpha, \beta) = \xi_8\Psi^2 + \{-\xi_4\Psi^+ + \xi_3\Psi^-\}/\xi_{11} \tag{6b}$$

$$\bar{Y}_{zy}(\alpha, \beta) = \xi_7\Psi^2 + \{\xi_2\Psi^+ - \xi_1\Psi^-\}/\xi_{10} \tag{6c}$$

$$\bar{Y}_{yz}(\alpha, \beta) = \xi_7\Psi^2 + \{\xi_4\xi_5\Psi^+ - \xi_3\xi_6\Psi^-\}/\xi_{11} \tag{6d}$$

$$\bar{Y}_{zz}(\alpha, \beta) = \xi_9\Psi^2 + \{-\xi_2\xi_5\Psi^+ + \xi_1\xi_6\Psi^-\}/\xi_{10} \tag{6e}$$

$$\Psi^2 = \cot(\gamma_2 h_2), \tag{6f}$$

$$\Psi^+ = \cot(\gamma_+ h_1), \tag{6g}$$

$$\Psi^- = \cot(\gamma_- h_1). \tag{6h}$$

The remaining constants appearing above, namely ξ_1 to ξ_{11}, can be related to constants multiplying the sine and cosine terms in field expressions inside the anisotropic and isotropic regions, as shown in [8] and [11].

To find the propagation constant, β, for the slot line, a Galerkin procedure similar to that of [9]–[11] is used to first expand the electric field components $\bar{E}_z$ and $\bar{E}_y$ within the slot in terms of known basis functions [11]. After the basis functions are substituted back into (6a), and appropriate inner products are performed, Parseval's theorem is applied to obtain a final set of algebraic matrix equations whose determinant contains β.

For the microstrip and edge coupled lines, a similar approach to the one used for the grounded slotline is implemented as well. Except that in this case, the impedance Green's function and the current basis functions on the metal strips are used instead. Notice that the edge coupled line is capable of supporting both even and odd modes. Therefore, appropriate choices for α, J_z, and J_y must be made accordingly during the computation of the propagation constant [7].

III. Results

To verify the theory presented in this paper, dispersive characteristics of the edge coupled microstrip line on a boron nitride substrate with $\epsilon_1 = 3.14$, $\epsilon_2 = \epsilon_3 = 5.12$, $\mu_{xx} = \mu_{yy} = \mu_{zz} = 1.0$ are computed and compared to the available results published in the literature. The physical dimensions of the guiding structure are

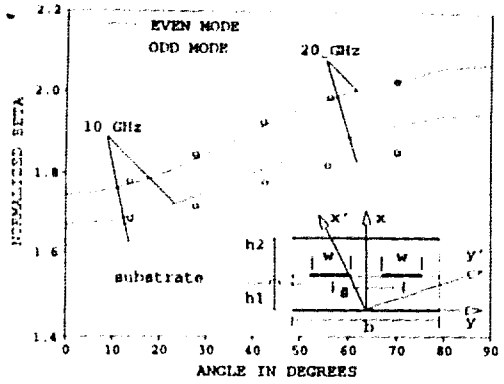

Fig. 1. Dispersion curves ($\beta - 0$) of the edge coupled line printed on boron nitride with $\epsilon_1 = 3.4$, $\epsilon_2 = 5.12$, $\epsilon_3 = 5.12$, $b = 8.5$ mm, $h_1 = 1.5$ mm, $h_2 = 3.0$ mm, $w = 1.5$ mm, and $S = 3.0$ mm. ---------- data computed by this method. ○ ○ ○ ○ ○ ○ data reproduced from [7].

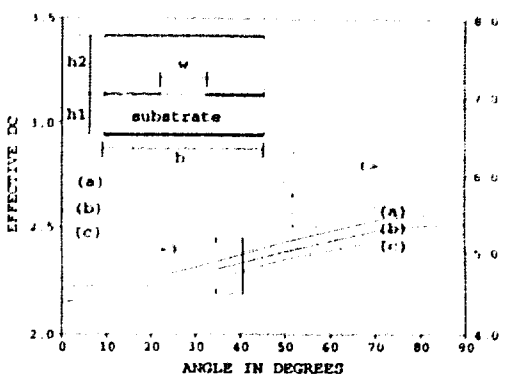

Fig. 2. Effective dielectric constant versus angle of the slotline on PTFE cloth ($\epsilon_1 = 2.45$, $\epsilon_2 = 2.89$, $\epsilon_3 = 2.95$ ——) and Glass cloth ($\epsilon_1 = 6.24$, $\epsilon_2 = 6.64$, $\epsilon_3 = 5.56$ · · · · · ·), with $\mu_{xx} = \mu_{yy} = \mu_{zz} = 1.0$, $b = 3.555$ mm, $h_1 = 0.254$ mm, $h_2 = 3.301$ mm, and $w = 0.254$ mm; at frequencies (a) 40 GHz, (b) 30 GHz, and (c) 20 GHz.

taken to be $b = 8.5$ mm, $h_1 = 1.5$ mm, $h_2 = 3.0$ mm, $w = 1.5$ mm, and $S = 3.0$ mm. Fig. 1 shows the normalized propagation constant β (β/k_o) plotted as a function of the rotation angle varying from 0° to 90° at frequencies of 10 and 20 GHz. Alongside the results computed by the method presented here are also the results from reference [7]; and as can be clearly seen, a good agreement between them is observed.

The effects of misalignment on the dispersive properties of transmission lines printed on biaxial substrates are studied next. The two chosen materials are the PTFE cloth and glass cloth. For the PTFE cloth when its principal axes are aligned with those of the waveguide, the material parameters characterizing the substrate are $\epsilon_1 = 2.45$, $\epsilon_2 = 2.89$, $\epsilon_3 = 2.95$, and $\mu_{xx} = \mu_{yy} = \mu_{zz} = 1.0$; while for the glass cloth, they are given by $\epsilon_1 = 6.24$, $\epsilon_2 = 6.64$, $\epsilon_3 = 5.56$, and $\mu_{xx} = \mu_{yy} = \mu_{zz} = 1.0$. Fig. 2 shows the response of the effective dielectric constant of the grounded slotline printed on the PTFE cloth and glass cloth, respectively. The physical dimensions of the structure used in computations are $b = 3.555$ mm, $h_1 = 0.254$ mm, $h_2 = 3.301$ mm, and $w = 0.254$ mm with the data calculated for angles of axes rotation changing from 0° to 90°, at three different frequencies. The dispersion curves follow a specific trend, indicating that as the frequency increases to 40 GHz, ϵ_{eff} increases correspondingly. An interesting observation can also be made by examining this figure more closely. It is apparent that even though ϵ_{eff} for the glass cloth is much larger than the one belonging to the PTFE cloth, the percentage of variation in ϵ_{eff} of the former due to the rotation angle is noticeably lower than for the latter. Such behavior can probably be attributed to the fact that the diagonal elements of the permittivity tensor for the glass cloth are nearly equal.

Fig. 3 displays the results for the microstrip line when the same cloth materials are used as substrates, with the dimensions of the structure given by $b = 12.7$ mm, $h_1 = 0.5$ mm, $h_2 = 12.2$ mm, and $w = 0.5$ mm. Once again, all computations were carried out at frequencies of 20 to 40 GHz, and the behavior of ϵ_{eff} is showing similar behavior patterns to those seen earlier for the slotline, including the lower sensitivity of the effective dielectric constant to angles of rotation for the glass cloth substrate.

The propagation properties of the edge coupled line on the PTFE cloth are examined next. The same permittivity tensor parameters (ϵ_1, ϵ_2, ϵ_3) are employed again with the pertinent dimensions of the structure given by $b = 7.0$ mm, $h_1 = 0.5$ mm, $h_2 = 3.0$ mm, and $w = 0.5$ mm. Fig. 4 illustrates the response of ϵ_{eff} to the rotation of the principal axes of the PTFE cloth (as a function of the strip spacing S) for odd and even modes, respectively. From these results it is apparent that as the spacing between the strips increases, ϵ_{eff} for both modes approaches the same limit, which implies that the two modes are essentially becoming degenerate.

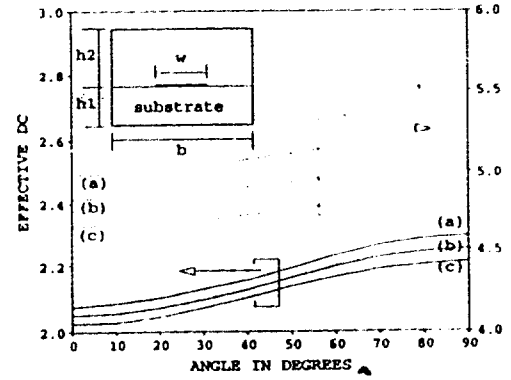

Fig. 3. Effective dielectric constant versus angle of the microstrip on PTFE cloth with ($\epsilon_1 = 2.45$, $\epsilon_2 = 2.89$, $\epsilon_3 = 2.95$ ——) and Glass cloth ($\epsilon_1 = 6.24$, $\epsilon_2 = 6.64$, $\epsilon_3 = 5.56$ · · · · · ·), with $\mu_{xx} = \mu_{yy} = \mu_{zz} = 1.0$, $b = 12.7$ mm, $h_1 = 0.5$ mm, $h_2 = 12.2$ mm, and $w = 0.5$ mm; at frequencies (a) 40 GHz, (b) 30 GHz, and (c) 20 GHz.

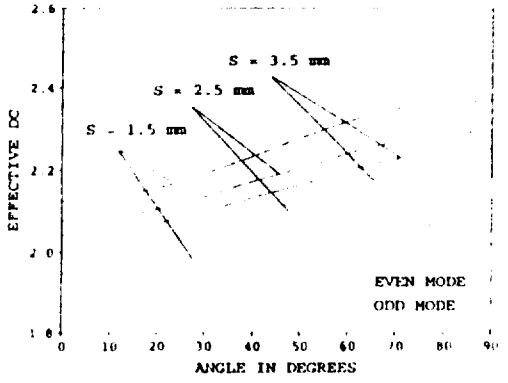

Fig. 4. Effective dielectric constant versus angle of the edge coupled line on PTFE cloth with $\epsilon_1 = 2.45$, $\epsilon_2 = 2.89$, $\epsilon_3 = 2.95$, $\mu_{xx} = \mu_{yy} = \mu_{zz} = 1.0$, $b = 7.0$ mm, $h_1 = 0.5$ mm, $h_2 = 3.0$ mm, $w = 0.5$ mm, and $f = 30$ GHz.

Finally, to illustrate how the tensor elements of the permeability would change the effective index of refraction under the rotation of the permittivity tensor, numerical results for the microstrip printed on a substrate that is characterized by both its biaxial [r]

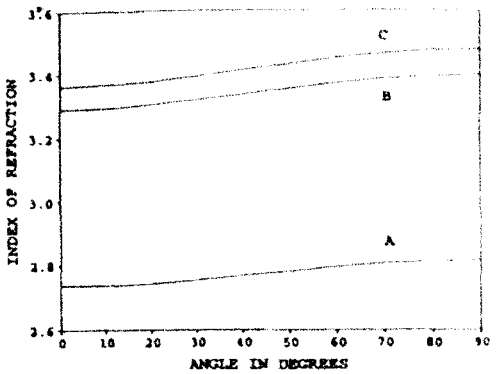

Fig. 5. Effective index of refraction versus angle of the microstrip with $\epsilon_1 = 9.6$, $\epsilon_2 = 10.4$, $\epsilon_3 = 8.2$, $b = 12.7$ mm, $h_1 = 0.5$ mm, $h_2 = 12.2$ mm, $w = 0.5$ mm, and $f = 30$ GHz. (A) $\mu_{xx} = \mu_{yy} = \mu_{zz} = 1.0$, (B) $\mu_{xx} = \mu_{zz} = 1.0$ and $\mu_{yy} = 1.6$, and (C) $\mu_{xx} = 1.0$, $\mu_{yy} = 1.6$, and $\mu_{zz} = 1.8$.

and $[\mu]$ are shown in Fig. 5. The physical dimensions of the guiding structure are the same as those used in earlier microstrip line studies, with the permittivity tensor parameters chosen to be $\epsilon_1 = 9.6$, $\epsilon_2 = 10.4$, and $\epsilon_3 = 8.2$. Dispersion curves A, B, and C show that by changing the material from being magnetically isotropic to magnetically biaxial can increase the effective index of refraction considerably, particularly by varying the μ_{yy} element.

IV. Conclusion

An analysis based on the spectral-domain method was applied to study the effects of misalignment between the principal axes of the substrate and those of the waveguide on the dispersive properties of grounded slotlines, microstrips, and edge coupled lines printed on anisotropic substrates. The newly derived expression for the Green's function is written explicitly in terms of both $[\epsilon]$ and $[\mu]$ tensor elements, with the off-diagonal elements of the permittivity also included in the formulation. The dispersion characteristics of these transmission lines are examined when they are printed on dielectrically biaxial substrates. Numerous results are provided for different medium parameters for frequencies up to 40.0 GHz when angles of axes rotation of the permittivity tensor change from 0° to 90°. Also, the variation in the index of refraction is examined for a microstrip line printed on a substrate which is characterized simultaneously by both its permittivity and permeability tensors. It is observed that misalignment effects on the dispersion properties of MIC's cannot be ignored, even at the lower frequencies for some anisotropic substrate materials.

References

[1] R. P. Owens, J. E. Itken, and T. C. Edwards, "Quasi-static characteristics of microstrip on an anisotropic sapphire substrate," *IEEE Trans. Microwave Theory Tech.*, vol. MTT-24, pp. 499-505, Aug. 1976.

[2] A-M. A. Al-Sherbiny, "Hybrid mode analysis of microstrip lines on anisotropic substrates," *IEEE Trans. Microwave Theory Tech.*, vol. MTT-29, pp. 1261-1265, Dec. 1981.

[3] N. G. Alexopoulos and C. M. Krowne, "Characteristics of single and coupled microstrips on anisotropic substrates," *IEEE Trans. Microwave Theory Tech.*, vol. MTT-26, pp. 387-393, June 1978.

[4] A. Nakatani and N. G. Alexopoulos, "Toward a generalized algorithm for the modeling of the dispersive properties of integrated circuit structures on anisotropic substrates," *IEEE Trans. Microwave Theory Tech.*, vol. MTT-33, pp. 1436-1441, Dec. 1985.

[5] H. Y. Yang and N. G. Alexopoulos, "Uniaxial and biaxial substrate effects of finline characteristics," *IEEE Trans. Microwave Theory Tech.*, vol. MTT-33, pp. 24-29, Jan. 1987.

[6] J. L. Tsalamengas, N. K. Uzunoglu, and N. G. Alexopoulos, "Propagation characteristics of a microstrip line printed on a general anisotropic substrate," *IEEE Trans. Microwave Theory Tech.*, vol. MTT-33, pp. 941-945, Oct. 1985.

[7] A. A. Mostafa, C. M. Krowne, and K. A. Zaki, "Numerical Spectral Matrix method for propagation in general layered media: application to isotropic and anisotropic substrates," *IEEE Trans. Microwave Theory Tech.*, vol. MTT-35, pp. 1399-1407, Dec. 1987.

[8] T. Q. Ho and B. Beker, "Spectral domain analysis of shielded microstrip lines on biaxially anisotropic substrates," *IEEE Trans. Microwave Theory Tech.*, vol. 39, pp. 1017-1021, June 1991.

[9] T. Itoh and R. Mittra, "A technique for computing dispersion characteristics of shielded microstrip lines," *IEEE Trans. Microwave Theory Tech.*, vol. MTT-22, pp. 896-898, Oct. 1974.

[10] L. Schmidt and T. Itoh, "Spectral domain analysis of dominant and higher order modes in finlines," *IEEE Trans. on Microwave Theory Tech.*, vol. MTT-28, pp. 981-985, Sept. 1980.

[11] T. Q. Ho, "Guided wave propagation in millimeter-wave integrated circuits using anisotropic materials," Ph.D. dissertation, University of South Carolina, Columbia, SC, Dec. 1991.

Analysis of an Infinite Array of Rectangular Anisotropic Dielectric Waveguides Using the Finite-Difference Method

Carlos Leônidas da Silva Souza Sobrinho and Attílio José Giarola

***Abstract*—The finite-difference method is used in the analysis of the propagation characteristics of an infinite array of rectangular dielectric waveguides. Particular attention is devoted to the mode coupling analysis and a comparison with results from an integral equation method is presented. The wave equation is solved in terms of the transverse components of the magnetic field, resulting in an eigenvalue problem with the elimination of spurious modes. The formulation is general and may be applied to the solution of other problems, including those with anisotropic dielectrics and with a continuous variation of the index of refraction profile in the waveguide cross section.**

I. Introduction

The practical application of dielectric waveguide in millimeter wave and optical integrated circuits depends critically on the propagation characteristics of these waveguides. For this reason, there has been increased interest in methods of determining these characteristics for practical dielectric waveguiding structures. The point-matching method was used to analyze the two-layer rectangular cross section waveguide [1]. The use of the finite-element method became attractive after the elimination of the spurious modes [2] and because of its potential of solving nonhomogeneous and anisotropic waveguides [3], [4]. The elimination of the spurious modes of the finite-difference method has also enhanced the

Manuscript received May 29, 1991; revised October 25, 1991. This work was partially supported by the following Brazilian agencies: CAPES, CNPq, TELEBRAS, and FINEP.

C. L. da Silva Souza Sobrinho is with the Electrical Engineering Department, Federal University of Para (UFPa), P.O. Box 918, CEP 66050, Belem, PA, Brazil.

A. J. Giarola is with School of Electrical Engineering, State University of Campinas (UNICAMP), P.O. Box 6101, CEP 13081, Campinas, SP, Brazil.

IEEE Log Number 9106223.